

2D simulation of laser plasma dynamics and radiation transfer into the target.

V.I. Mazhukin, S.G. Gorbachenko

Institute of Mathematical Modeling, Russian Academy of Sciences, Miusskaya sq. 4A, 125047, Moscow, Russia

I. Smurov

Ecole Nationale d'Ingenieurs de Saint-Etienne, 58 rue Jean Parot, 42023, Saint-Etienne Cedex, France

G. Flamant

Institute of Science et de Genie des Materiaux et Procedes, C.N.R.S., 66125 Font-Romeu Cedex, France

A. Gleizes

Universite Paul Sabatier, 118 route de Narbonne, 31062 Toulouse Cedex, France

Summary

The results of computer modeling are presented concerning the laser action on the metal target in the air and Al vapour environment. It is established, that the dominant mechanism of the plasma development for the considered regimes is the propagation of ionisation wave.

1. Introduction

Enhanced interest to pulse laser action on various materials is related to solution of a number of practically important problems [1]. In most cases, laser action on condensed medium leads to onset of evaporation and subsequent plasma formation in evaporated substance. Gaseous medium can substantially screen the irradiated surface depending on environmental conditions, fluency and pulse duration. In some cases [2] the plasma screening becomes dominant phenomenon. Due to complexity and interdependence of processes in plasma it becomes important to determine role of the dominant processes and factors: gas dynamic expansion, radiation transfer, ionisation degree of gaseous media and absorption of laser radiation. This objective can be achieved by means of mathematical modeling of developed plasma in the frame of 2D radiative gas dynamics. Previously [3], the influence of the laser radiation wavelength and initial conditions on plasma evolution has been studied.

In the present paper the processes in erosive plasma of aluminium vapour and air plasma are comparatively analysed. The transmissivity value is determined numerically, that is indicative on conversion of laser radiation to emissive radiation of plasma, and simultaneous action of two fluxes on the surface.

2. Physical set-up and governing equations.

Let us consider aluminium target placed into cold gaseous medium initially transparent for laser radiation, and thin hot gaseous layer adjacent to the target surface. Laser radiation propagates along the z -axis directed along the target surface normal. One fraction of the laser energy is absorbed by the hot layer and the other by the target surface.

Laser plasma, emerging near the target in the evaporated substance or environmental gas, is characterised by strong spatial variation of density ρ and temperature T resulted from appreciable hydrodynamic phenomena. Therefore in most cases the laser plasma has variable optical thickness, and reabsorption and radiation transfer processes become important, if geometrical sizes of plasma cloud are large enough. The plasma of variable optical density is the most complicated for investigations. Two different phenomena: hydrodynamic expansion (compression) and radiation transfer contribute comparably to energy balance of the system. Mathematical description of these phenomena in plasma is usually performed by means of Radiative Gas Dynamics (RGD) model.

The model is based on the following assumptions:

- i) plasma is considered to be the absorbing medium (excluding elastic scattering);
- ii) plasma is described in non-viscous non-heat-conductive gas approximation;
- iii) Local Thermodynamic Equilibrium (LTE) conditions are fulfilled in all points of the plasma domain.

Under these assumptions the problem can be formulated as follows. The condensed medium is described by non-linear boundary value problem for heat transfer equation:

$$\rho C_p(T) \frac{\partial T}{\partial t} = \frac{1}{r} \frac{\partial}{\partial r} \left(r \lambda(T) \frac{\partial T}{\partial r} \right) + \frac{\partial}{\partial z} \left(\lambda(T) \frac{\partial T}{\partial z} \right) \quad (1)$$

$$0 < r < L, \quad 0 < z < z_0$$

where C_p , λ , ρ are specific heat, thermal conductivity and density of the target.

The processes in gaseous medium are described by the unsteady Radiative Gas Dynamics (RGD) equation system. In cylindrical co-ordinate system with axial symmetry the governing equations are written as:

$$\frac{\partial \rho}{\partial t} + \frac{1}{r} \frac{\partial}{\partial r} (r \rho u) + \frac{\partial}{\partial z} (\rho v) = 0, \quad (2)$$

$$\frac{\partial \rho u}{\partial t} + \frac{1}{r} \frac{\partial}{\partial r} (r \rho u^2) + \frac{\partial}{\partial z} (\rho u v) = - \frac{\partial (p + \omega)}{\partial r}, \quad (3)$$

$$\frac{\partial \rho v}{\partial t} + \frac{1}{r} \frac{\partial}{\partial r} (r \rho u v) + \frac{\partial}{\partial z} (\rho v^2) = - \frac{\partial (p + \omega)}{\partial z} \quad (4)$$

$$\frac{\partial \rho \varepsilon}{\partial t} + \frac{1}{r} \frac{\partial}{\partial r} (r \rho u \varepsilon) + \frac{\partial}{\partial z} (\rho v \varepsilon) = -p \left[\frac{1}{r} \frac{\partial (ru)}{\partial r} + \frac{\partial v}{\partial z} \right] - \frac{1}{r} \frac{\partial W_r}{\partial r} - \frac{\partial W_z}{\partial z} - \frac{\partial G}{\partial z}, \quad (5)$$

$$p = p(\rho, T), \quad \varepsilon = \varepsilon(\rho, T), \quad (6)$$

$$\bar{\Omega} \text{grad } I_v + \kappa_v I_v = \kappa_v I_{eq}, \quad (7)$$

$$\bar{W} = \int_0^\infty d\nu \int \bar{\Omega} I_\nu d\Omega, \quad \kappa_\nu = \kappa_\nu(\nu, \rho, T), \quad (8)$$

$$\frac{\partial G^+}{\partial z} + \kappa_l G^+ = 0, \quad \frac{\partial G^-}{\partial z} - \kappa_l G^- = 0, \quad G = G^+ + G^-, \quad (9)$$

$$0 < r < L, \quad z_0 < z < M$$

where u, v are flow velocity components along r -axis and z -axis; \bar{W}, W_r, W_z are full radiation flow and its components; ε and p are internal energy and pressure of the plasma; κ_l is absorption of the laser radiation; G, G^+, G^- are full intensity of laser radiation and intensities of forward-directed and reflected waves of the laser radiation; κ_ν, I_ν denote spectral absorption and spectral intensity of the plasma radiation; ν, Ω are frequency and direction of photon.

In the equation system (2) is continuity equation, (3),(4) are momentum transfer equations along r -axis and z -axis, (5) is internal energy balance, (6) are equations of state, (7) is radiation transfer equation, (8) is radiative flow equation, (9) is transfer equation for laser radiation.

The charge composition of plasma is described by non-linear equation system of Saha [4],[5].

$$\frac{N_e \sum_{m=0}^{M^{z+1}} N_m^{z+1}}{\sum_{m=0}^{M^z} N_m^z} = \frac{g_e g^{z+1}}{g^z} \left\{ \frac{m T}{2\pi \hbar^2} \right\}^{3/2} \exp\left[-\frac{J^z}{T}\right], \quad z = 0, 1, \dots, Z_{\max} \quad (10)$$

Absorption coefficient of laser radiation κ_l is determined as [4],[5]:

$$\kappa_l = \frac{8\pi e^6}{3mhc(6\pi mk)^{1/2}} \frac{N_e \sum z^2 N^z}{\sqrt{3} T^{1/2}} \left(1 - \exp\left(-\frac{h\nu}{kT}\right) \right) \quad (11)$$

The equation system (2)-(11) is supplemented by the following boundary conditions on the phase interface. The target surface is assumed to be non-ablating and to be influenced by the laser G , and the radiation W , flows:

$$-\lambda \frac{\partial T}{\partial z} = G_s + W_s - \sigma T_s^4. \quad (12)$$

The other boundaries of the target are assumed to be heat impermeable:

$$\lambda \frac{\partial T}{\partial r} = \lambda \frac{\partial T}{\partial z} = 0 \quad (13)$$

For gas dynamics and radiation transfer equations the following boundary conditions are used:

$$\begin{aligned}
 z = z_0 : \quad & u = 0, \quad W_s = W_z = cU / 2, \\
 & G_s = A(T_s)G^+, \quad G^- = (1 - A(T_s))G^+; \\
 r = 0 : \quad & v = 0, \quad W_r = 0; \\
 z = M : \quad & p = p_0, \quad W_z = -cU / 2, \quad G^+ = G; \\
 r = N : \quad & p = p_0, \quad W_r = -cU / 2.
 \end{aligned}
 \tag{14}$$

Radiative losses of plasma consist of continuous and linear spectrum losses. Continuous radiation includes contribution from bremsstrahlung, photorecombination as well as bielectronic recombination processes. Linear radiation forms under spontan decay of excited states. Absorption of plasma is determined by all these processes and such a way its value depend on frequency ν , density ρ , and temperature T .

Spectral absorption $\kappa(\nu, \rho, T)$, as well as equations of state $p(\rho, T)$ and $\varepsilon(\rho, T)$ are evaluated in advance for pre-defined ranges of T and ρ . The evaluation is based on solution of self-adjusted field equations (method of Hartree-Fock-Slater). For subsequent application in multi-group procedure for continuous radiation transfer, the obtained values are averaged within each group using Plank method. The calculation results are then saved in three-dimensional tables for $\kappa_i(\nu, \rho_i, T_n)$ and two-dimensional for $p_i(\rho_i, T_n)$, $\varepsilon_i(\rho_i, T_n)$. The i , n , k indexes refer to rows, columns and layers (groups) of tabulated values.

Main peculiarities of RGD computations are due to radiation transfer equation (7). The solution depends not only on the temperature and density, but additionally on photon frequency ν and direction $\bar{\Omega}$. The larger dimensionality of radiation transfer equation system complicates numerical treatment of RGD problem as a whole. The difficulty can be successfully overcome if special averaging procedure is applied, that permits to reduce dimensionality of radiation transfer.

For elimination of frequency dependence multi-group approximation is used. The total frequency range $\nu \in [0, \infty]$ is divided onto finite number of intervals (groups) $\sum_{k=1}^N [\nu_k, \nu_{k+1}]$. For each group the absorption κ_k is assumed to be independent on photon energy. At the assumption, the transfer equation (7), plasma radiation flux W , energy density U and radiation intensity are rewritten as:

$$\begin{aligned}
 \bar{\Omega} \text{grad} I_k + \kappa_k I_k &= \kappa_k I_{\text{eq},k}, \\
 \bar{W} &= \int_0^\infty d\nu \int \bar{\Omega} I_\nu d\Omega = \sum_{k=1}^N \int \bar{\Omega}_k I_k d\Omega_k, \\
 I_k &= \int_{\nu_k}^{\nu_{k+1}} I_\nu d\nu, \quad U = \frac{1}{c} \int_0^\infty \nu d\nu = \sum_{k=1}^N \int \Omega I_k d\Omega.
 \end{aligned}
 \tag{15}$$

For elimination of dependence on angular variable Ω we apply so-called diffusion model [6]. According to this approach multi-group transfer equation (15) can be presented as:

$$\begin{aligned}
\frac{1}{r} \frac{\partial (rW_r)_k}{\partial r} + \frac{\partial W_{z,k}}{\partial z} + \kappa_k c U_k &= 4\sigma_k \kappa_k T^4, \\
\frac{c}{3} \frac{\partial U_k}{\partial r} + \kappa_k W_{r,k} &= 0, \\
\frac{c}{3} \frac{\partial U_k}{\partial z} + \kappa_k W_{z,k} &= 0, \quad k = 1, 2, \dots, N.
\end{aligned} \tag{16}$$

3. Results and analysis.

In computational experiments the laser action on metal target in air and Al vapour environment is considered. The ambient pressure of both media is set to 1bar. The initial temperatures of the air and Al vapour are equal to 300K and 0.2eV respectively, that is approximately match the evaporation temperatures on the outer side of Knudsen layer at normal conditions. The initial densities are equal to $\rho_{\text{air}}=1.25 \times 10^{-3} \text{ g/cm}^3$, $\rho_{\text{Al}}=1.4 \times 10^{-3} \text{ g/cm}^3$. The initial region of optical breakdown is treated as thin layer of hot plasma ($\Delta z=5 \times 10^{-3} \text{ cm}$, $\Delta r=2.4 \times R_f$, $T=1 \text{ eV}$) placed along the irradiated surface of the target. The temporal - spatial distribution of laser pulse intensity is chosen to be product of two Gaussian:

$$\begin{aligned}
G &= G_0 \exp\left(-\frac{r^2}{R_f^2}\right) \exp\left(-\frac{t^2}{\tau^2}\right), \quad -\infty < t < \infty, \quad 0 < r < L, \\
G_0 &= 5 \times 10^9 \text{ W/cm}^2, \quad \tau = 10^{-8} \text{ s}, \quad R_f = 0.25 \text{ cm}.
\end{aligned}$$

The mathematical modeling have permitted to reveal the peculiarities of laser plasma development under action of ultra-short laser pulses. In general there are three mechanisms of energy dissipation and transfer in laser plasma evolution, namely, ionisation of gaseous medium, work of compression forces and transfer of plasma intrinsic radiation. Characteristic feature of ultra-short action is that the ionisation mechanism dominates over all the period of laser action. This results in fast propagation of ionisation wave toward the radiation source and fast heating of gaseous medium without appreciable gas-dynamic effects being observed. Depicted on figs. 1-4 are 2D spatial distribution of temperature T and density ρ at the onset of laser pulse $t=-4.9 \text{ ns}$ (figs 1,2) and after the pulse termination $t=30 \text{ ns}$ (figs. 3,4). The temperature of the hot region achieves maximum $T_{\text{max}}=6.5 \text{ eV}$. However, variation of gas-dynamic and radiative components is insignificant, that is observed on density plot, fig. 2. The maximum pressure of the hot region reaches approximately 1.5kbar, that leads to the onset of gas-dynamic expansion. At the time $t=30 \text{ ns}$ the density of the hot region falls down approximately by one order of magnitude, fig. 4. The size of disturbed region along the z -axis ($\Delta z \approx 0.6 \text{ cm}$) becomes comparable to initial size of the hot region.

The pattern of the processes evolution is qualitatively the same while considering Al vapour environment. Again, the ionisation wave is appeared to be the dominant factor of plasma propagation. However the propagation velocity in the Al vapour differs substantially from that in the air due to difference of optical and spectroscopy characteristics of two media. At the middle of the pulse $t \approx 0.1 \text{ ns}$, the ionisation front locates at $z \approx 2.5 \text{ cm}$, figs. 5,6. Such the

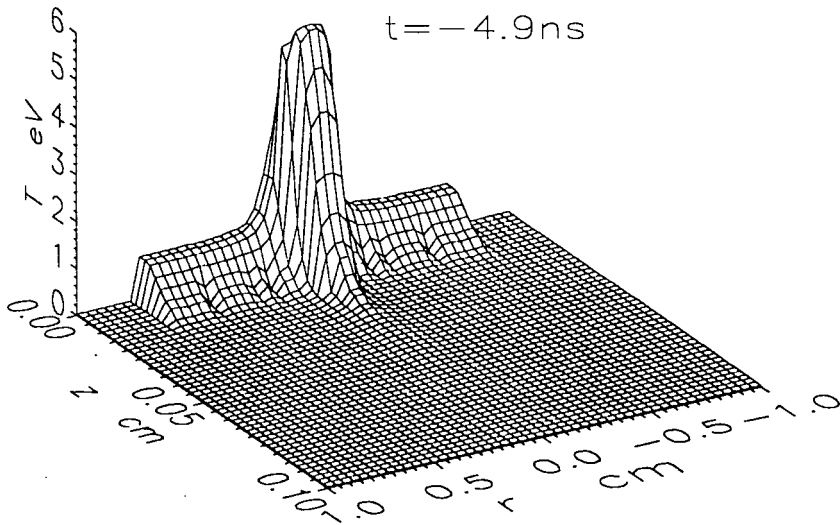


Figure 1. 2D spatial distribution of temperature T at the $t = -4.9 \text{ ns}$ for the air plasma.

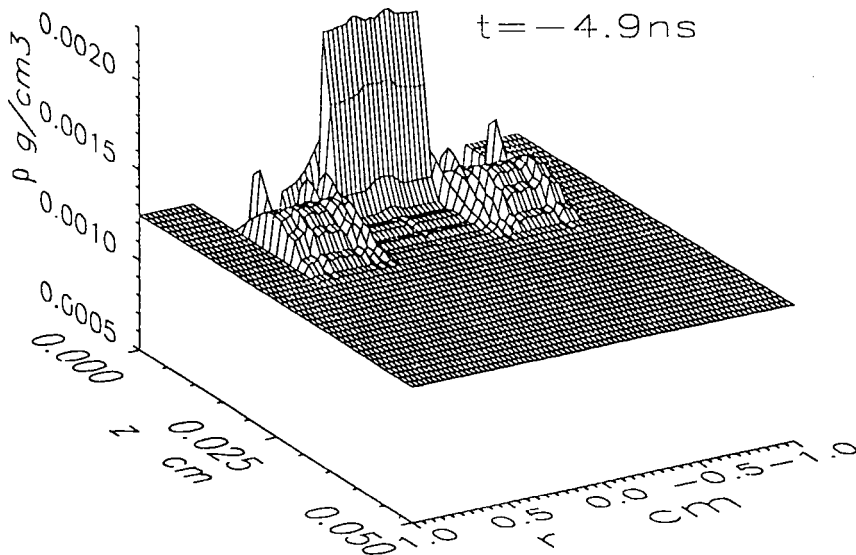


Figure 2. 2D spatial distribution of density ρ at the $t = -4.9 \text{ ns}$ for the air plasma.

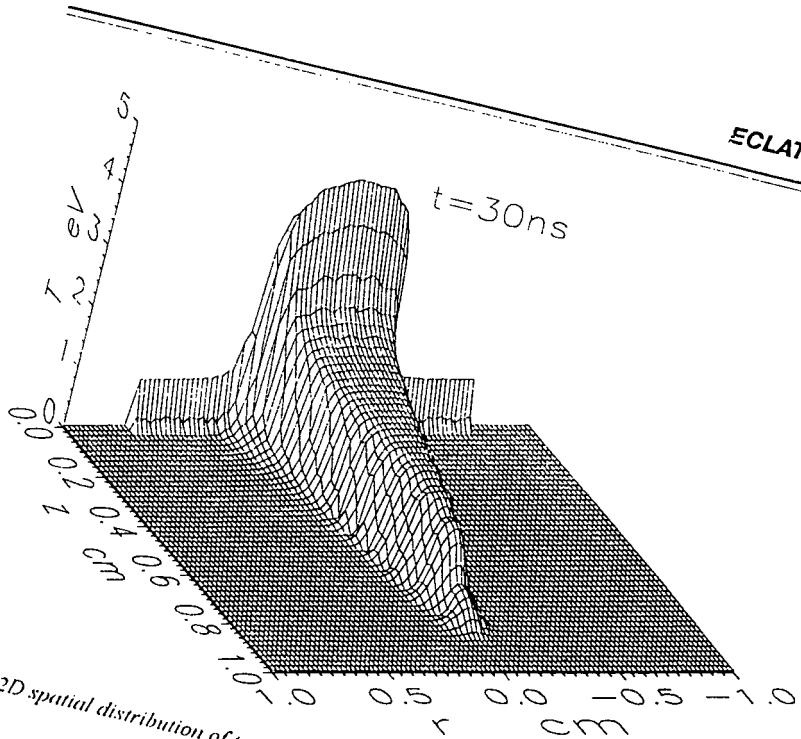


Figure 3. 2D spatial distribution of temperature T at the $t=30\text{ns}$ for the air plasma.

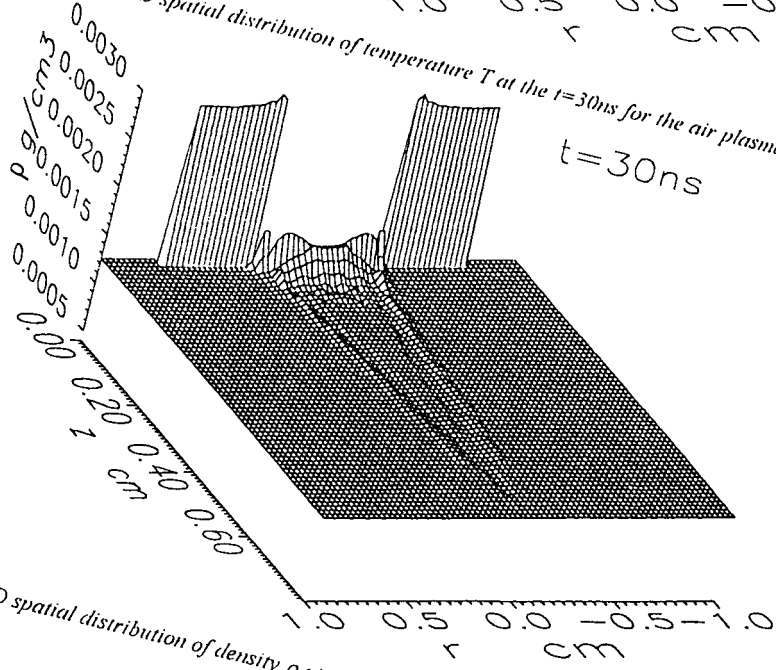


Figure 4. 2D spatial distribution of density ρ at the $t=30\text{ns}$ for the air plasma.

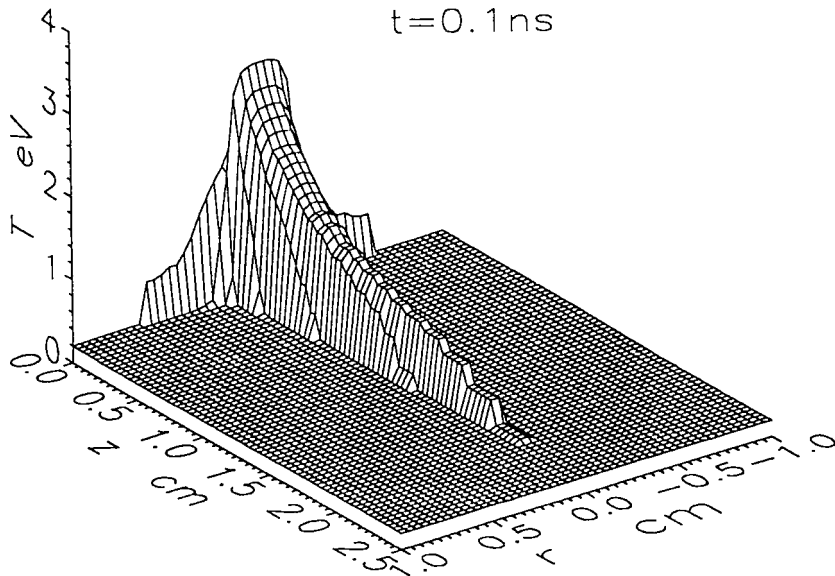


Figure 5. 2D spatial distribution of temperature T at the $t=0.1$ ns for the Al vapour plasma.

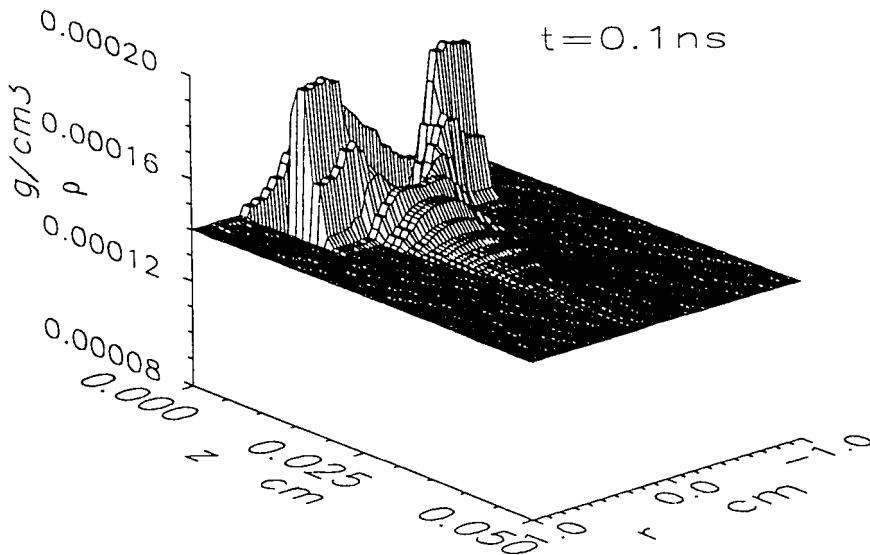


Figure 6. 2D spatial distribution of density ρ at the $t=0.1$ ns for the Al vapour plasma.

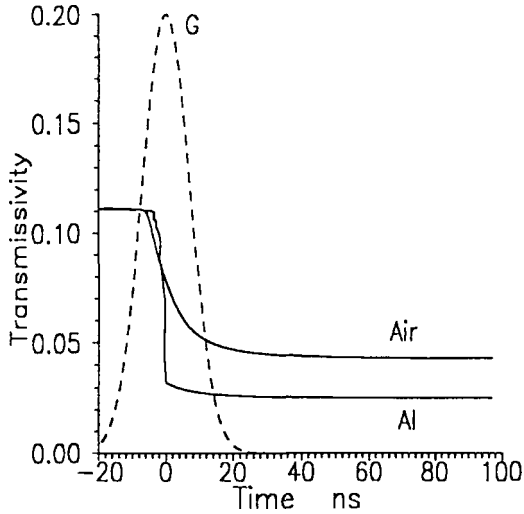


Figure 7. Time history of transmissivity $Tr(t)$ (solid line) and intensity of incident laser radiation $G(t)$ for the air and Al vapour plasma.

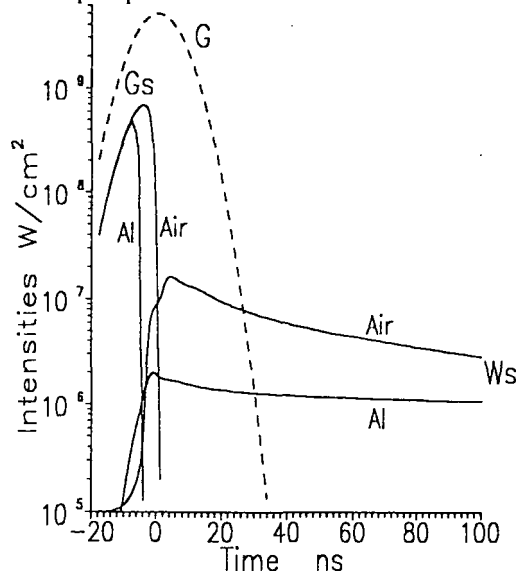


Figure 8. Time history of laser radiation flux on the target surface $G_s(t)$, plasma radiation flux $W_s(t)$ and intensity of incident laser radiation $G(t)$ for the air and Al vapour plasma.

fast propagation of plasma front leads to increase of the size of plasma cloud, and subsequently, to decrease of the maximum temperature, $T_{\max} \approx 3.4 \text{ eV}$. The large size of Al vapour plasma results in optical thickness of the cloud being greater than one of the air plasma, despite the higher temperature and density of the latter plasma. The assertion is confirmed by analysis of transmissivity of the laser radiation, that is defined as

$$T_r(t) = \frac{\int_{-\infty}^t d\tau \int_{-L}^L (G_s(r, \tau) + W_s(r, \tau)) ds}{\int_{-\infty}^t d\tau \int_{-L}^L G(r, \tau) ds},$$

and is presented on fig. 7 for the both media. The transmissivity values relate to strongly reflecting targets with $A_s < 0.2$. Presented on fig. 8 are time histories of radiation fluxes G , and W_s , at the target surface.

Conclusion.

The results of mathematical modeling indicates i) strong non-linear coupling between thermal, radiative and gas-dynamics processes in laser plasma; ii) appreciable change of pattern of physical processes on transition from microsecond to nanosecond range of pulse duration.

References

- [1]. G.Gallies, H. Schittenhelm, P. Berger, F. Dausinger, H. Hugel, Time-resolved diagnostics of energy-coupling during material processing with excimer lasers, SPIE, v. 2246, pp. 126-135, 1994.
- [2]. J. Hermann, A.L.Thomann, C.Boulmer-Leborgne, B.Dubreuil, M.L.De Giorgi, A.Perrone, A. Luches, I.N.Mihailescu, Plasma diagnostics in pulsed laser TiN layer deposition, J.Appl. Phys., v. 77, p. 2928, 1995
- [3]. V.I. Mazhukin, I. Smurov, G. Flamant, 2D-simulation of the system: laser beam + laser plasma + target, Applied Surface Science, v. 86, pp. 303-309, 1996.
- [4]. Ya. B. Zeldovich, Yu. P. Raizer, Physics of shock waves and high-temperature hydrodynamic phenomena (in Russian), Science, Moscow, 1966.
- [5]. Reactions under plasma conditions, Ed. by M. Venugopalan, v. I, Wiley-Interscience, 1970.
- [6]. V.I.Mazhukin, I. Smurov, G. Flamant, Simulation of laser plasma dynamics: influence of ambient pressure and intensity of laser radiation, J. Comp. Phys., v. 112 pp.78-90, 1994.